

# 4

## Special Loudspeaker Drivers for Low-frequency Bandwidth Extension

The preceding chapter dealt with low-frequency BWE exclusively through signal-processing algorithms. For the case of small loudspeakers, it was shown that non-linear processing could enhance the perception of very low frequency tones. The advantage of such an approach is that the loudspeaker need not be modified in any way, as the algorithm is tailored to the loudspeaker. In this chapter, two options are described whereby modifying the loudspeaker driver can also lead to enhanced bass perception. This is achieved by modifying the force factor of the driver, typically by employing either a very strong or a very weak magnet, compared to what is commonly used in typical drivers. Both these approaches also require some pre-processing of the signal before it is applied to the modified loudspeaker. Thus, this kind of BWE is a mixed approach combining mechanical and algorithmic measures. In Sec. 4.1, the influence of the force factor on the performance of the loudspeaker is reviewed, after which Secs. 4.2–4.3 discuss high force factor and low force factor drivers, respectively, and their required signal processing. Section 4.4 presents an analysis of the transient responses of these special drivers.

### 4.1 THE FORCE FACTOR

Direct-radiator loudspeakers typically have a very low efficiency, since the acoustic load on the diaphragm or cone is relatively low compared to the mechanical load, and in addition the driving mechanism of a voice coil is quite inefficient in converting electrical energy into mechanical motion. The drivers have a magnetic structure – which determines the force factor  $Bl$  – that is deliberately kept at an intermediate level so that the typical response is flat enough to use the device without significant equalization. It was already shown in Sec. 1.3.2.3 that the force factor  $Bl$  plays an important role in loudspeaker design; it determines among others the frequency response, the transient response, the electrical input impedance, the cost, and the weight; we will discuss various of these consequences. To show the influence on the frequency response, the sound pressure level

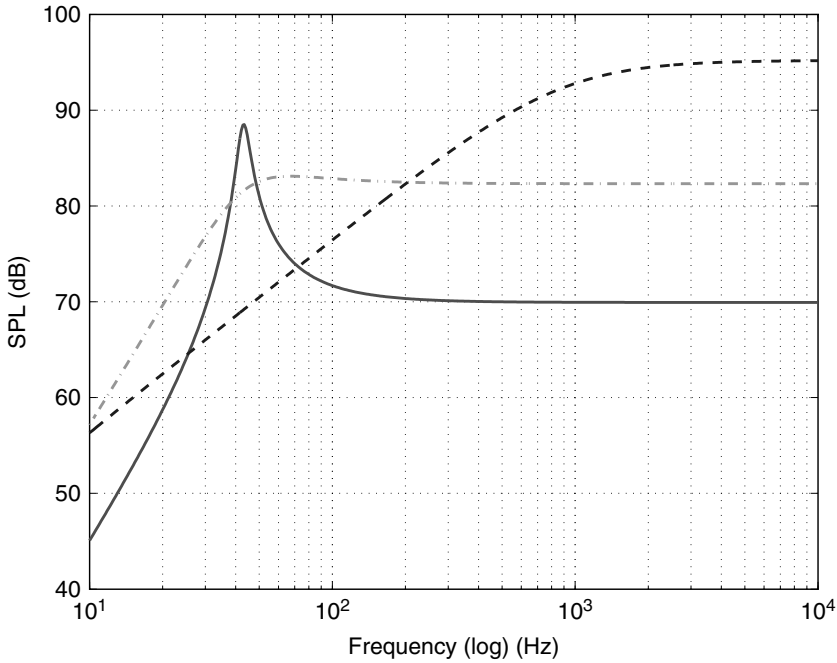


**Figure 4.1** Sound pressure level (SPL) for the driver MM3c with three  $Bl$  values (low, medium, and high), while all other parameters are kept the same (1-W input power),  $Bl = 1.2$  (solid),  $Bl = 5$  (dash-dot), and  $Bl = 22$  (dash). See Table 4.2 for the other parameters

(SPL) of a driver with three  $Bl$  values (low, medium, and high) is plotted in Fig. 4.1, while all other parameters are kept the same. It appears that the curves change drastically for varying  $Bl$ . The most prominent difference is the shape, but the difference in level at high frequencies is also apparent. While the low- $Bl$  driver has the highest response at the resonance frequency, it has a poor response beyond resonance, which requires special treatment, as discussed in Sec. 4.3.1. The high- $Bl$  driver has a good response at higher frequencies, but a poor response at lower frequencies, which requires special equalization as discussed in Sec. 4.2. In between, we have the well-known curve for a medium- $Bl$  driver. To show the influence of  $Bl$  on the electrical input impedance, the magnitude is plotted for a driver with two  $Bl$  values (low and medium), while all other parameters are kept the same, see Fig. 4.2. In this plot, the curve for  $Bl = 22$  is omitted; it has similar shape, but a much higher  $Q$  and a larger peak (at  $R_e + Bl^2/R_t = 2206 \Omega$ ). It also appears that these curves change drastically for varying  $Bl$ . The phase of the electrical input impedance is plotted in Fig. 4.3. The underlying reason for the importance of  $Bl$  is that besides determining the driving force, it also gives (electric) damping to the system. The total damping is equal to the (real part of the) radiation impedance, the mechanical damping, and the electrical damping ( $(Bl)^2/R_e$ ), where the electrical one dominates for medium- and high- $Bl$  loudspeakers, and is most prominent around the

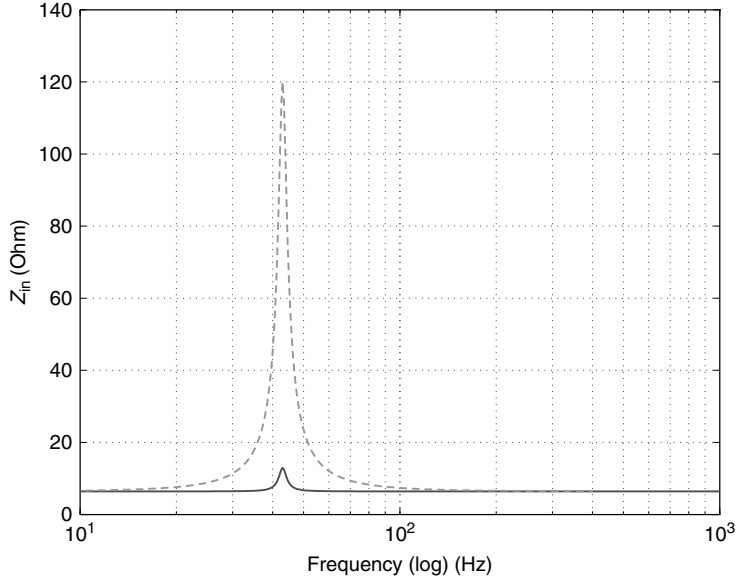


**Figure 4.2** The electrical input impedance for the driver MM3c with two  $Bl$  values (low, and medium, respectively  $Bl = 1.2$  (solid), and  $Bl = 5$  (dash)), while all other parameters are kept the same ( $L_e = 0$ ). See Table 4.2 for the other parameters

resonance frequency. The power efficiency given in Eqn. 1.54 can be written as

$$\eta = \frac{(Bl)^2 R_r}{R_e \{(R_m + R_r)^2 + (R_m + R_r)(Bl)^2 / R_e + (m_t \omega_0 v)^2\}}, \quad (4.1)$$

clearly showing the influence of  $Bl$ . This importance is further elucidated in the following paragraph.

**A dimensionless measure of damping** In Vanderkooy *et al.* [284], a dimensionless parameter was introduced to describe the relative damping due to  $Bl$ . As  $Bl$  increases, the box and suspension restoring forces become less relevant, as we shall see later, so we choose a parameter of the form

$$\frac{i\omega(Bl)^2 / R_e}{-\omega^2 m_t}, \quad (4.2)$$

which is the ratio of the electrical damping force to the inertial force on the total moving mass  $m_t$  (consisting of the cone with its air load). We remove the imaginary unit and the negative sign, so the relative damping factor becomes

$$\delta = \frac{(Bl)^2}{\omega_r m R_e}. \quad (4.3)$$

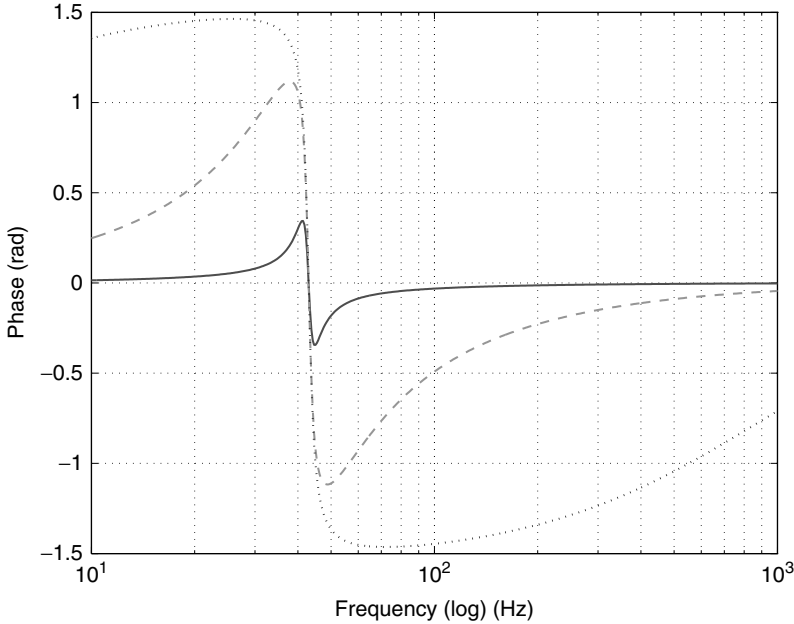


**Figure 4.3** The phase [rad] of the electrical input impedance for the driver MM3c with three  $Bl$  values (low, and medium, and high, while all other parameters are kept the same (1-W input power),  $Bl = 1.2$  (solid),  $Bl = 5$  (dash), and  $Bl = 22$  (dots). See Table 4.2 for the other parameters

The frequency  $\omega_t$  can be chosen to represent the low-frequency end of the intended audio spectrum, or it could be set to a reference frequency such as 50 Hz, or the resonance frequency  $\omega_0$ . The reference frequency may be useful since the low-frequency cut-off of a system is significantly altered when  $Bl$  is significantly increased. Incidentally, for the usual Butterworth system aligned to frequency  $\omega_0$ ,  $\delta$  would be  $\sqrt{2}$ . The drivers MM3c and HBI mentioned in Table 4.2 have  $\delta = 0.059$  and  $\delta = 4.43$  respectively. The common parameter  $Q_e$ , the electrical  $Q$ -factor, while similar to  $\delta^{-1}$  (and at the resonance frequency there holds  $Q_e = \delta^{-1}$ ), is predicated on a normal driver for which the resonance frequency is determined by the interaction between inertial and suspension forces. As  $Bl$  is increased, the suspension forces are less relevant, and Eqn. 4.3 is a better measure than  $Q_e$ .

## 4.2 HIGH FORCE FACTOR DRIVERS

In the 1990s, a new rare-earth-based material, neodymium-iron-boron (NdFeB), in sintered form, came into more common use. It has a very high flux density coupled with a high coercive force, possessing a  $B$ - $H$  product increased by almost an order of magnitude compared to more common materials. This allows drivers to be built in with much larger total magnetic flux, thereby increasing  $Bl$  by a large factor. In Vanderkooy *et al.* [284], some features of normal sealed-box loudspeakers with greatly increased  $Bl$  were outlined.

This work focused mainly on the efficiency of the system as applied to several amplifier types, but also indicated several other avenues of interest. Figure 4.1 shows the frequency response curves (using Eqns. 1.39 and 1.40) for three  $Bl$  values: 1.2, 5.0, and 22 N/A. At the higher- $Bl$  value, the electromagnetic damping is very high. If we ignore in this case the small mechanical and acoustic damping of the driver, the damping term is proportional to  $(Bl)^2/R_e$ . For a Butterworth response, the inertial term  $\omega^2 m$ , the damping term  $\omega(Bl)^2/R_e$ , and total spring constant  $k_t$  are all about the same at the bass cut-off frequency. When  $Bl$  is increased by a factor of 5, the damping is increased by a factor of 25. Thus the inertial factor, which must dominate at high frequencies, becomes equal to the damping at a frequency about 25 times higher than the original cut-off frequency. This causes the flat response of the system to have a 6-dB per octave roll-off below that frequency, as shown in the figure.

At very low frequencies, the spring-restoring force becomes important relative to the damping force at a frequency 25 times lower than the original cut-off frequency. Below this the roll-off is 12 dB/octave. Such frequencies are too low to influence audio performance, but it is clear that the system (driver and cabinet) is now no longer constraining the low-frequency performance. We could use a much smaller box without serious consequences.

How much smaller can the box be? The low-frequency cut-off has been moved down by a factor of nearly 25. The suspension stiffness  $k$  is small, and since  $k_B \propto 1/V_0$ , the cut-off frequency will return to the initial bass cut-off frequency when the box size is reduced by a factor of about 25: a 25-litre box could be reduced to 1 litre. Powerful electrodynamic damping has allowed the box to be reduced in volume without sacrificing the response at audio frequencies. The only penalty is that we must apply some equalization.

The equalization needed to restore the response to the original value can be deduced from Fig. 4.1, since the required equalization is the difference between  $Bl = 5$  (dashed), and  $Bl = 22$  (dotted) curves. Such equalization will, in virtually all cases, increase the voltage applied to the loudspeaker, since audio energy resides principally at lower frequencies. The curve levels out at just over 12 dB at low frequencies, but in actual use one might attenuate frequencies below, say, 40 Hz.

The power efficiency for very large  $Bl$  can be calculated (using Eqn. 4.1) as

$$\lim_{Bl \rightarrow \infty} \eta = \frac{R_r}{R_m + R_r}. \quad (4.4)$$

This clearly shows that the efficiency increases for decreased mechanical damping  $R_m$ .

**An observation about equalization** The required equalization can be calculated by the frequency response ratio  $H_L(\omega)/H_H(\omega)$  using Eqn. 1.40, where the subscripts refer to the high and low values of  $Bl$ . The required equalization function for two loudspeakers with different  $Bl$  values, but identical in all other respects, can also be calculated using an alternative approach, giving new insight, which we develop now.

For the two loudspeakers to produce the same acoustic output, the shape and motion of the two pistons (or cones) must be the same. Since all other aspects of the loudspeakers are the same, this can be achieved if the total force on the pistons is the same, thus ensuring that they have the same motion. The force is derived from the electromagnetic

Lorentz force,  $BlI(\omega)$ . Since current  $I(\omega) = V(\omega)/Z(\omega)$ , where  $V(\omega)$  is the loudspeaker voltage and  $Z(\omega)$  is its electrical impedance, we must arrange to have  $BlV(\omega)/Z(\omega)$  the same for the two conditions. Hence

$$\frac{Bl_H V_H(\omega)}{Z_H(\omega)} = \frac{Bl_L V_L(\omega)}{Z_L(\omega)}. \quad (4.5)$$

Note, however, that since

$$H_{EQ}(\omega) = V_H(\omega)/V_L(\omega), \quad (4.6)$$

then

$$H_{EQ}(\omega) = \frac{Bl_L/Z_L(\omega)}{Bl_H/Z_H(\omega)}, \quad (4.7)$$

a very simple relationship that indicates the importance of the electrical impedance and the force factor  $Bl$  in determining loudspeaker characteristics. We can verify the result using Eqns. 1.40 and 1.42. Note that it applies to the response at any orientation, not just on-axis, and represents a general property of acoustic transducers with magnetic drivers.

### 4.3 LOW FORCE FACTOR DRIVERS

The introduction of concepts such as Flat-TV and small (mobile) sound reproduction systems has led to a renewed interest in obtaining a high sound output from compact loudspeaker arrangements with a good efficiency. Compact relates here to both the volume of the cabinet into which the loudspeaker is mounted, as well as the cone area of the loudspeaker. Normally, low-frequency sound reproduction with small transducers is quite inefficient. To increase the efficiency, the low-frequency region, say 20 to 120 Hz can be mapped to a single tone, and by using a special transducer with a low- $Bl$  value, at a very high efficiency at that particular tone. In the following section, an optimal force factor will be derived to obtain such a result.

#### 4.3.1 OPTIMAL FORCE FACTOR

The solution to obtain a high sound output from a compact loudspeaker arrangement, with a good efficiency, consists of two steps. First, the requirement that the frequency response must be flat is relaxed. By making the magnet considerably smaller (See Fig. 4.6 at the left side), a large peak in the SPL curve (see Fig. 4.1 (solid curve)) will appear. Since the magnet can be considerably smaller than usual, the loudspeaker can be of the moving magnet type with a stationary coil (see Fig. 4.6 and Fig. 4.7), instead of vice versa. At the resonance frequency, the efficiency can be a factor of 10 higher than that of a normal loudspeaker. In this case we have, at the resonance frequency of about 40 Hz, an SPL of almost 90 dB at 1-W input power, even when using a small cabinet. Since it is operating in resonance mode only, the moving mass can be enlarged (which might be necessary owing to the small cabinet), without degrading the efficiency of the system. Owing to the large and narrow peak in the frequency response, the normal operating

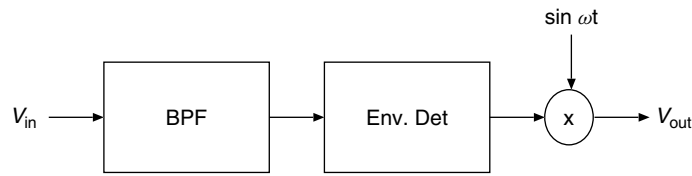


**Figure 4.4** Frequency mapping scheme. The box labeled ‘BPF’ is a band pass filter, and ‘Env. Det.’ is an envelope detector, the signal  $V_{out}$  is fed (via a power amplifier) to the driver

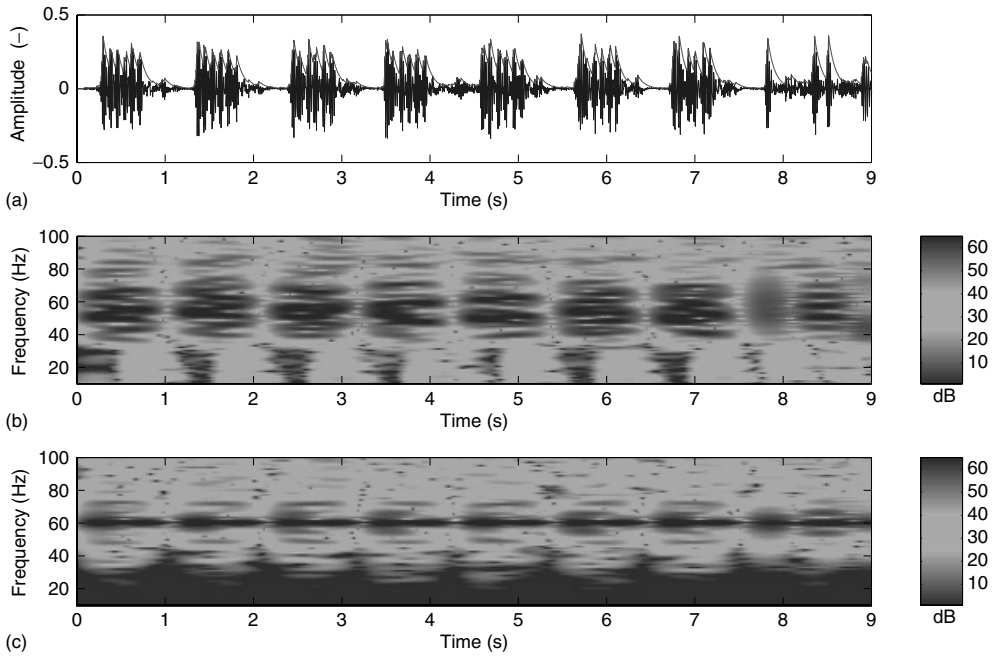


**Figure 4.5** The signals before and after the frequency-mapping-processing of Fig. 4.4. (a) Shows the signal at  $V_{in}$ , and the output of the envelope detector as the thin outline along  $V_{in}$ . (b) and (c) Show the spectrogram of the input and output signals respectively

range of the driver decreases considerably, however. This makes the driver unsuitable for normal use. To overcome this, a second measure is applied. The low-frequency content of the music signal, say 20 to 120 Hz, is mapped to a slowly amplitude-modulated tone whose frequency equals the resonance frequency of the transducer. This can be done with a set-up depicted in Fig. 4.4. The modulation is chosen such that the coarse structure (the envelope) of the music signal after the mapping is the same as before the mapping, which is shown in Fig. 4.5. Part (a) shows the waveform of a rock-music excerpt (the blue curve); the red curve depicts its envelope. Parts (b) and (c) show the spectrograms of the input and output signals respectively, clearly showing that the frequency bandwidth of



**Figure 4.6** Left: Magnet system of the prototype (MM3c shown in Fig. 4.7) of the optimal low- $Bl$  driver (only 3 g and 4.5-mm diameter) with a 50 Euro cent coin. Right: a small woofer of 13-cm diameter and about 1 kg

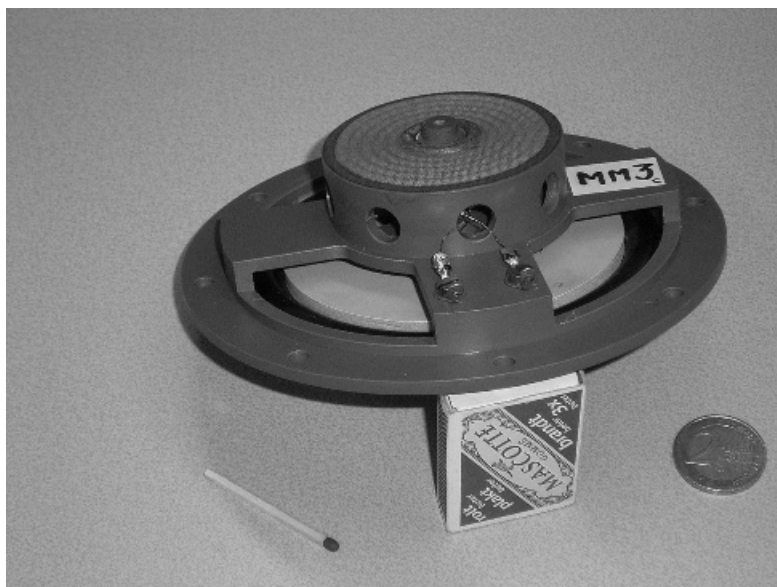


**Figure 4.7** Picture of the prototype driver (MM3c) with a 2 Euro coin and ordinary matches. At the position where a normal loudspeaker has its heavy and expensive magnet, the prototype driver has an almost empty cavity; only a small moving magnet is necessary, which is visible at Fig. 4.6 (left side)



the signal around 50 Hz decreases after the mapping, yet the temporal modulations remain the same. Using Eqns. 1.37 and 1.39, the voltage sensitivity at the resonance frequency can be written as

$$H(\omega = \omega_0) = \frac{j\omega_0 S B l \rho}{2\pi r R_e (R_m + (Bl)^2/R_e)}. \quad (4.8)$$

If Eqn. 4.8 is maximized by adjusting the force factor  $Bl$  (differentiating  $H(\omega = \omega_0)$  with respect to  $Bl$  and setting  $\partial H/\partial(Bl) = 0$ ), we get

$$\frac{(Bl)^2}{R_e} = R_m. \quad (4.9)$$

Note at this point that if Eqn. 4.9 holds, we get for this particular case  $Q_e = Q_m$  (see Eqn. 1.43). It appears that the maximum voltage sensitivity is reached as the electrical damping term  $(Bl)^2/R_e$  is equal to the mechanical damping term  $R_m$ ; in this case, we refer to the optimal force factor as  $(Bl)_o$ . If Eqn. 4.9 is substituted into Eqn. 4.8, this yields the optimal voltage sensitivity ratio

$$H_o(\omega = \omega_0) = \frac{j\omega\rho S}{4\pi r (Bl)_o}. \quad (4.10)$$

We find that the specific relationship between  $(Bl)_o$  and both  $R_m$  and  $R_e$  (Eqn. 4.9) causes  $H_o$  to be inversely proportional to  $(Bl)_o$  (which may seem counterintuitive), and thus also inversely proportional to  $\sqrt{R_m}$ . The power efficiency at the resonance frequency for the optimality condition obtained by substitution of Eqn. 4.9 into Eqn. 4.1 yields

$$\eta_o(\omega = \omega_0) = \frac{R_m R_r}{(R_m + R_r)^2 + (R_m + R_r) R_m}. \quad (4.11)$$

This can be approximated for  $R_r \ll R_m$  as

$$\eta_o(\omega = \omega_0) \approx \frac{R_r}{2R_m}, \quad (4.12)$$

which clearly shows that for a high-power efficiency at the resonance frequency, the cone area must be large, since  $R_r$  is – according Eqn. 1.47 – proportional to the squared cone area; and that the mechanical damping must be as small as possible. This conclusion is the same as for achieving a high voltage sensitivity (given by Eqn. 4.1).

Using Eqn. 1.39, 1.40, and  $v = dx/dt$ , we get for the cone velocity

$$\frac{v(\omega = \omega_0, (Bl)^2/R_e = R_m)}{V_{in}} = \frac{1}{2(Bl)_o}, \quad (4.13)$$

which again shows the benefit of low  $Bl$  and  $R_m$  values. Further, we get, assuming the optimality condition given by Eqn. 4.9 and using Eqn. 1.45,

$$Z_{in}(\omega = \omega_0, (Bl)^2/R_e = R_m) \approx 2R_e. \quad (4.14)$$

## 4.4 TRANSIENT RESPONSE

In order to calculate the transient behaviour of the system, we calculate the transient response of a driver. We will determine the response to a sinusoid that is switched on at  $t = 0$ , and finally, the impulse response.

### 4.4.1 GATED SINUSOID RESPONSE

The response of a driver, with resonance frequency  $\omega_0$ , to a sinusoidal signal with frequency  $\omega_s$ , switched on at  $t = 0$

$$v(t) = \begin{cases} 0, & t < 0 \\ A \sin(\omega_s t), & t \geq 0 \end{cases} \quad (4.15)$$

is calculated. It is convenient to write Eqn. 4.15 in the Laplace domain

$$V(s) = \frac{A\omega_s}{s^2 + \omega_s^2}. \quad (4.16)$$

The transfer function  $H(s)$  from voltage  $V$  to excursion  $X$  is

$$H(s) = \frac{1}{s^2 m_t + s R_t + k_t}, \quad (4.17)$$

where  $m_t$  is the total moving mass,  $R_t$  is the total damping (mechanical, electrical, and acoustical)

$$R_t = R_m + \frac{(Bl)^2}{R_e} + R_a, \quad (4.18)$$

and  $k_t$  the total spring constant, as described in Sec. 1.3.2.3. Hence  $X(s)$  can be calculated as

$$X(s) = \frac{\frac{Bl}{R_e} \frac{A\omega_s}{s^2 + \omega_s^2}}{s^2 m_t + s R_t + k_t}. \quad (4.19)$$

Assuming that Eqn. 4.17 has complex poles (this is the case if  $R_t^2 < 4m_t k_t$ ), they are at

$$s_{1,2} = -\beta\omega_0 \pm i\omega_n = -a \pm ib. \quad (4.20)$$

By using partial fraction expansion (see e.g. Palm [198], or Arfken and Weber [21]), we can write Eqn. 4.19 as sum of basic terms, and then the inverse Laplace transformation can be readily carried out, resulting in

$$x(t) = \frac{Bl\omega_s A}{m_t R_e} \left[ e^{-at} \left( k_1 \cos \omega_n t + \left( \frac{k_2 - ak_1}{\omega_n} \right) \sin \omega_n t \right) + k_3 \cos \omega_s t + \frac{k_4}{\omega_s} \sin \omega_s t \right], \quad (4.21)$$

where

$$\begin{aligned}
 a &= \frac{R_t}{2m_t}, \\
 b^2 &= \omega_n^2 = \frac{k_t}{m_t} - \left( \frac{R_t}{2m_t} \right)^2, \\
 k_1 &= \frac{2a}{\Delta}, \\
 k_2 &= \frac{3a^2 - b^2 + \omega_s^2}{\Delta}, \\
 k_3 &= -k_1, \\
 k_4 &= \frac{a^2 + b^2 - \omega_s^2}{\Delta}, \\
 \Delta &= (a^2 + b^2)^2 + 2\omega_s^2(a^2 - b^2) + \omega_s^4,
 \end{aligned} \tag{4.22}$$

where we identify  $a^2 + b^2 = \sqrt{\frac{k_t}{m_t}} = \omega_0^2$  as the driver's resonance frequency, and

$$\begin{aligned}
 \beta &= \frac{R_t}{2\sqrt{m_t k_t}}, \\
 Q &= \frac{\sqrt{m_t k_t}}{R_t},
 \end{aligned} \tag{4.23}$$

as the driver's damping and quality factor  $Q$ , respectively. Further, we see that  $2\beta = Q^{-1}$ . Looking at Eqn. 4.21, it is clear that the time constant of the transient behaviour is determined by  $a^{-1}$ . It is proportional to the moving mass  $m_t$ , and must be small in order to get a fast response. As a special case, we consider  $\omega_s = \omega_0$ , that is, the driver is actuated at its resonance frequency. Furthermore, we assume that the transient part (the product with  $e^{-at}$  in Eqn. 4.21) has faded away. Then, Eqn. 4.21 reduces to

$$x(t) = -\frac{ABl}{\omega_s R_e R_t} \cos \omega_s t. \tag{4.24}$$

Here, we see that there is a  $3\pi/4$  phase shift between the input voltage (see Eqn. 4.15) and the output excursion.

For various drivers, the lumped-element parameters are determined and listed in Table 4.2. For three of those drivers (see Table 4.1), the response to a suddenly switched sinusoid (see Eqn. 4.15) is calculated (using Eqn. 4.21). The results are shown in Fig. 4.8 for the low- $Bl$  driver and the case that the driving signal is equal to the resonance frequency  $f_0 = 43$  Hz, in Fig. 4.9 for a driving signal of 47 Hz, and in Fig. 4.10 for a driving signal of 86 Hz. For the two other drivers, with a medium- and high- $Bl$  respectively, transient responses at resonance frequency are shown in Figs. 4.11 and 4.12 (responses at other frequencies are very similar for these two drivers). These results show that the medium- and high- $Bl$  driver systems rapidly converge to their steady-state response, while this is not the case for the low- $Bl$  driver system. Also, the medium- and high- $Bl$  driver systems are not sensitive to deviations of the input frequency, while, again, this is not the case for the low- $Bl$  driver system. This is especially obvious in Fig. 4.10, where in the first half of the time interval,

**Table 4.1** Legend to the transient responses plotted in Figs. 4.8 – 4.12 of various drivers: low-*Bl* (MM3c), normal-*Bl* (AD70652), and high-*Bl* (HBI) loudspeakers. The frequency  $f_s$  of the gated sinusoid was set to three different values relative to the resonance frequency  $f_0$  of the driver:  $f_0$ ,  $1.1f_0$ , and  $2f_0$ . In all cases, the amplitude was 1 V. For the entries labeled ‘–’ no figures are included, since these are similar to the other figure referred to in the same column. The details of the lumped-element parameters are listed in Table 4.2

	MM3c	AD70652	HBI
$f_s = f_0$	Fig. 4.8	Fig. 4.11	Fig. 4.12
$f_s = 1.1f_0$	Fig. 4.9	–	–
$f_s = 2f_0$	Fig. 4.10	–	–
$Bl$	1.2	6.5	22
$Q_e$	17	0.61	0.22

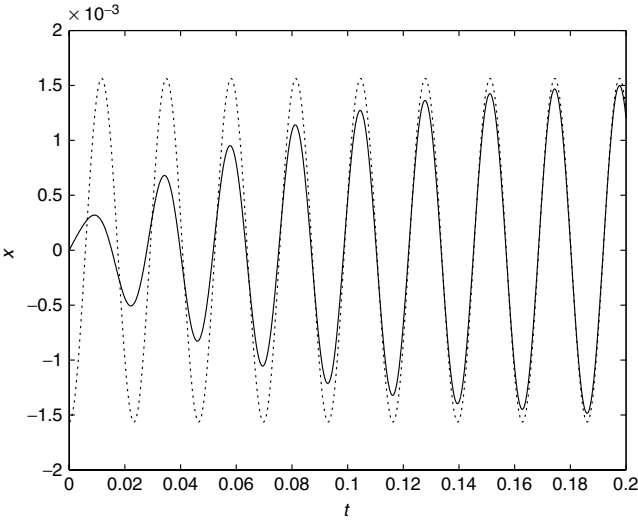


**Figure 4.8** The displacement (solid line) of the low-*Bl* prototype driver MM3c (using Eqn. 4.21). The lumped-element parameters are listed in Table 4.2. The frequency of the driving signal  $f_s$  is equal to driver’s resonance frequency  $f_0 = 43$  Hz. The dotted line is the stationary value of the displacement (Eqn. 4.21 for  $\lim_{t \rightarrow \infty}$ )

there is significant interference between the terms with  $\omega_n$  and  $\omega_s$  of Eqn. 4.21, leading to severe amplitude modulation during the onset transient. Therefore, the low-*Bl* driver should only be used at (or near) resonance frequency.

#### 4.4.2 IMPULSE RESPONSE

The impulse response  $h(t)$  can be calculated directly (again under the assumption that  $R_t^2 < 4m_t k_t$ ), by the inverse Laplace transform of  $H(s)$  (Eqn. 4.17) as

$$h(t) = \frac{\omega_0}{\omega_n} e^{-at} \sin(\omega_n t + \phi), \tag{4.25}$$

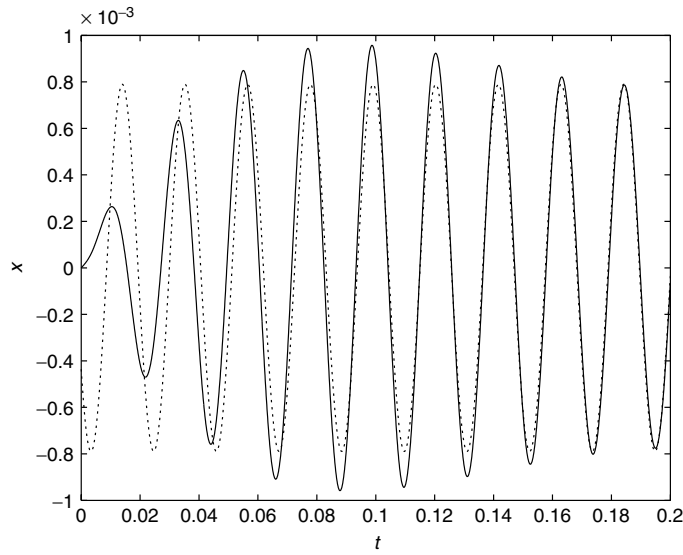


**Figure 4.9** The displacement (solid line) of the low- $BI$  prototype driver MM3c (using Eqn. 4.21). The lumped-element parameters are listed in Table 4.2. The frequency of the driving signal  $f_s$  is equal to 47 Hz, which is 1.1 times the driver's resonance frequency  $f_0 = 43$  Hz. The dotted line is the stationary value of the displacement (Eqn. 4.21 for  $\lim_{t \rightarrow \infty}$ )

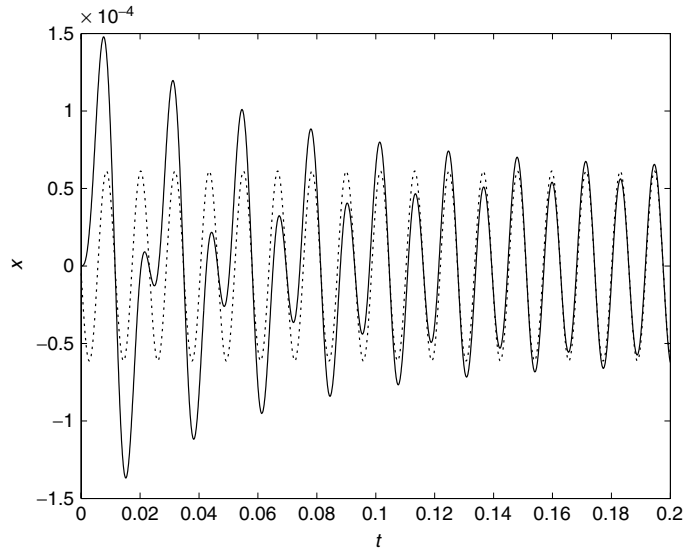


**Figure 4.10** The displacement (solid line) of the low- $BI$  prototype driver MM3c (using Eqn. 4.21). The lumped-element parameters are listed in Table 4.2. The frequency of the driving signal  $f_s$  is equal to 86 Hz, which is twice the driver's resonance frequency  $f_0 = 43$  Hz. The dotted line is the stationary value of the displacement (Eqn. 4.21 for  $\lim_{t \rightarrow \infty}$ )

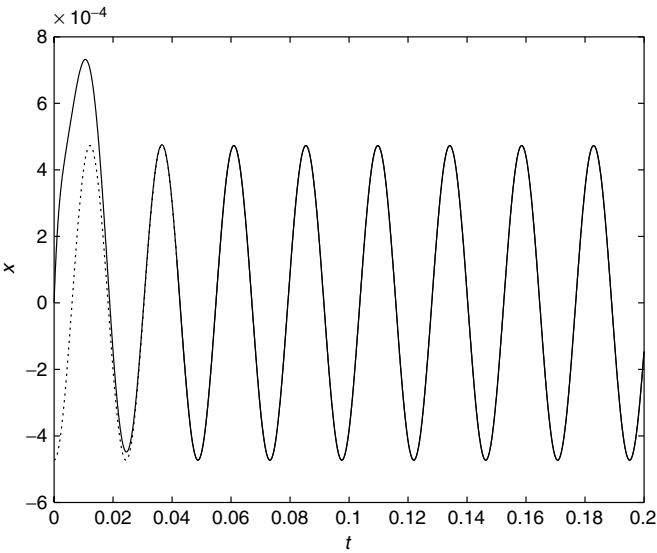


**Figure 4.11** The displacement (solid line) of the medium-*BI* driver (using Eqn. 4.21). The lumped-element parameters are listed in Table 4.2. The frequency of the driving signal  $f_s$  is equal to driver's resonance frequency  $f_0 = 41$  Hz. The dotted line is the stationary value of the displacement (Eqn. 4.21 for  $\lim_{t \rightarrow \infty}$ )

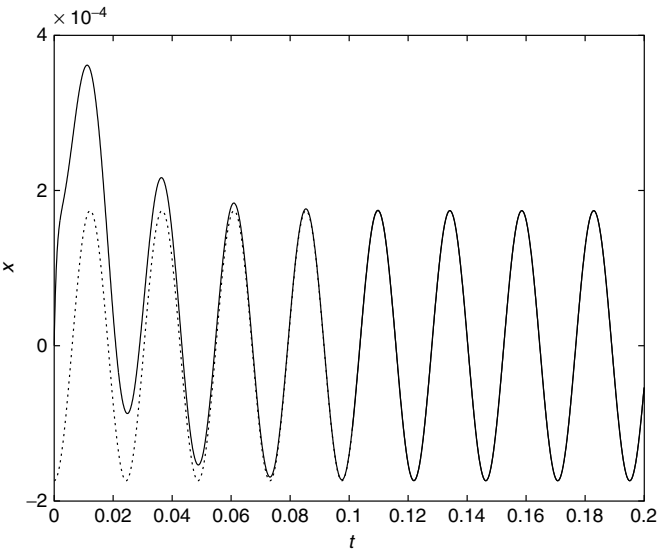


**Figure 4.12** The displacement (solid line) of a high-*BI* driver (HBI), (using Eqn. 4.21). The lumped-element parameters are listed in Table 4.2. The frequency of the driving signal  $f_s$  is equal to driver's resonance frequency  $f_0 = 41$  Hz. The dotted line is the stationary value of the displacement (Eqn. 4.21 for  $\lim_{t \rightarrow \infty}$ )

where  $\phi = \arctan(b/a)$ . Here, we see again that the time constant  $a^{-1}$  (the ratio  $2m_t/R_t$ ) must be small to get a fast response (decay).

#### 4.5 DETAILS OF LUMPED-ELEMENT PARAMETERS AND EFFICIENCY

The lumped parameters for some loudspeakers are given in Table 4.2. From these values and Eqn. 1.54, the efficiency  $\eta$  is calculated and plotted in Fig. 4.13, showing that the efficiency is in the range of 0.2 to 10%. As a rule of thumb, we see from Table 4.2 that for woofers  $k$  is equal to about 1 N/mm, and that  $R_m \approx 1$  Ns/m, while the other parameters may differ significantly between the various drivers.

The equivalent volume of a loudspeaker is given by

$$V_{eq} = \rho c^2 (\pi a^2)^2 / k_t. \quad (4.26)$$

Alternatively, for a given volume of the enclosure, the corresponding  $k_t$  of the ‘air-spring’ can be calculated. Mounting a loudspeaker in a cabinet will increase the total spring constant by an amount given by Eqn. 4.26, and subsequently increase the bass cut-off frequency of the system. To compensate for this bass loss, the moving mass has to be increased; thus  $\sqrt{k_t m}$  is increased, which changes  $Q_e$  (see Eqn. 1.43). Then  $Bl$  must be increased in order to preserve its original value. The original frequency response is then maintained, but at the cost of a more expensive magnet and a loss in efficiency. This is the designer’s dilemma: high efficiency or small enclosure? To meet the demand for a certain cut-off frequency, the enclosure volume must be greater. Alternatively, the

**Table 4.2** The lumped parameters for various low-frequency loudspeakers (woofers). A 4 in., and some 7, 8, 10, and 12 in. drivers, each of them with a low and high  $Q_e$ . Further, two special drivers, a (optimal) low- $Bl$  (MM3c) and a high- $Bl$  one (HBI). The former is an experimental driver (see Fig. 4.6 for its compact magnet system together with a more classical driver, and Fig. 4.7 for the whole driver). The high- $Bl$  one (HBI) is discussed in Vanderkooy *et al.* [284]. See Table 1.2 for the abbreviations and the meaning of the variables

Type	$R_e$ $\Omega$	$Bl$ Tm	$k$ N/m	$m_t$ gr.	$R_m$ Ns/m	$S$ cm <sup>2</sup>	$f_0$ Hz	$Q_m$	$Q_e$
AD44510	6.6	3.5	839	4	0.86	54	72	2.2	1.02
AD70652	7.5	6.5	885	13.2	1.48	123	41	2.3	0.61
AD70801	6.9	2.9	1075	6.3	0.81	123	66	3.2	2.13
AD80110	6.0	9.0	971	16.5	1.38	200	39	2.9	0.29
AD80605	6.8	5.1	1205	13.4	0.84	200	48	4.8	1.05
AD10250	6.6	13.0	1124	38.5	2.74	315	27	2.4	0.25
AD10600	6.8	5.9	909	28.5	1.06	315	29	4.8	0.99
AD12250	6.6	13.0	1429	54.0	2.93	490	26	3.0	0.34
AD12600	6.9	6.0	1205	33.0	0.76	490	31	8.2	1.21
MM3c	6.4	1.2	1022	14.0	0.22	86	43	17.0	17.00
HBI	7.5	22.0	3716	56.0	0.91	490	41	16.0	0.22

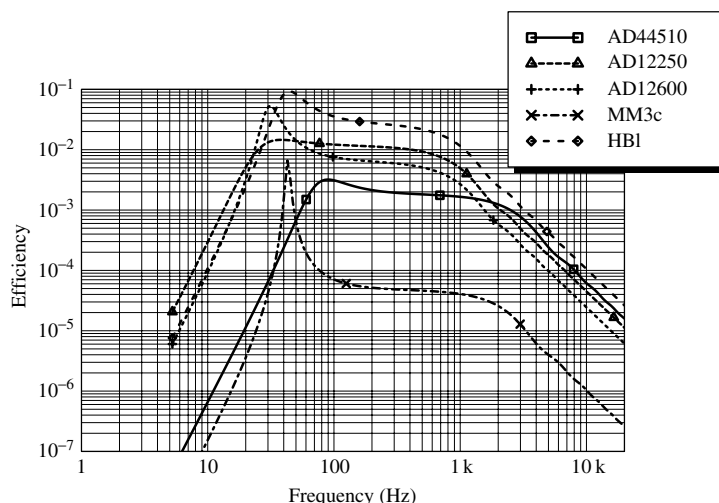


**Figure 4.13** Efficiency of various loudspeakers: AD44510 (solid/square markers), AD12250 (dashed/triangle markers), AD12600 (small-dashed/‘+’ markers), MM3c (dot-dashed/‘x’ markers), and HBI (wide-dashed/‘◇’ markers). See Table 4.2 for the parameters. Note that not all drivers have the same cone area

efficiency for a given volume will be less than that for a system with a higher cut-off frequency. This dilemma is (partially) solved by using the low- $B_I$  concept as discussed in Sec. 4.3, however, at the expense of a slightly decreased sound quality and some additional electronics to accomplish the frequency mapping. The decrease of sound quality appears to be modest, apparently because the auditory system is less sensitive at low frequencies (Sec. 1.4.5.2). Also, the other parts of the audio spectrum have a distracting influence on this mapping effect, which has been confirmed in a study by Le Goff *et al.* [158], in which detectability of mistuned fundamental frequencies were determined for a variety of realistic complex signals.

## 4.6 DISCUSSION

In the previous sections we have seen that the force factor  $B_I$  plays a very important role in loudspeaker design. It determines the efficiency, the impedance, the SPL response, the temporal response, the weight, and the cost. The choice concerning these parameters depends on the application. If the size of the cabinet is of less importance, a medium  $B_I$  is the simplest solution, since it does not require any other measures. On the other hand, if a small cabinet and a high efficiency are important than the low  $B_I$  system with an optimum value given by Eqn. 4.9 has the preference. This requires special electronics, however. Also, the transient response is less favorable than that of a larger magnet system and this makes it less suitable for High-Fi applications. The high  $B_I$  is in between: it has a high efficiency and good response, but it requires an expensive magnet and additional electronics. Clearly, the application dictates the parameter choice.